

INTERNATIONAL UNION OF  
PURE AND APPLIED CHEMISTRY  
MACROMOLECULAR DIVISION

**A COLLABORATIVE STUDY OF  
THE DYNAMIC MECHANICAL  
AND IMPACT PROPERTIES  
OF PVC—II**

*A Report of the IUPAC Working Party on 'Structure and  
Properties of Commercial Polymers'*

*Prepared for publication by*  
A. GONZE and J. C. CHAUFFOUREAUX  
Solvay and Cie, Brussels, Belgium

LONDON  
BUTTERWORTHS

315

## A COLLABORATIVE STUDY OF THE DYNAMIC MECHANICAL AND IMPACT PROPERTIES OF PVC

### ABSTRACT

The paper summarizes the work done by a working party of IUPAC on dynamic mechanical, tensile and impact properties of a rigid and a toughened PVC. Storage modulus and loss factor of both PVCs have been measured over a wide range of temperatures and frequencies in torsion pendulum and flexural vibration tests. A secondary transition of PVC and the glass transition associated with the CPE present in the toughened PVC have been located with fairly good agreement between the five participants. Charpy, falling weight, Izod, tensile and prestressed impact tests have been utilized over a wide range of temperature to study impact properties. The brittle-tough transition temperature range of both PVCs has been located for each test method and the results were discussed.

Tensile properties of both PVCs were specially studied in the linear range of deformation, at yield point and at rupture. Yield stress measurements are in good agreement with the generalized Eyring theory proposed by Bauwens-Crowet. Rupture strains show two transition zones; the first one, associated with a tough-brittle process, has the same activation energy as the secondary transition found by dynamic mechanical measurements; the second one, associated with a tough-tough process, seems to be strongly correlated with thermal dissipation in test pieces.

The relaxation modulus of each PVC has been calculated over eight decades of time at several temperatures from 20 to 64°C on the basis of dynamic mechanical, tensile modulus and stress relaxation measurements.

The identity of the activation energy measured for the transition zones by means of dynamic mechanical, tensile and impact tests respectively shows that the molecular relaxation processes measured in the linear range of deformation of PVC, have a strong effect on the impact or tensile properties.

---

### INTRODUCTION

The present paper covers the second part of a work done by an IUPAC Working Party, under the chairmanship of J. W. Barrett, on the dynamic mechanical and impact properties of a rigid (normal) and a toughened polyvinyl chloride (PVC). The objective of the work was to study the effect of molecular parameters of polymers on those properties.

The first part of the work on PVC was published in *Pure and Applied Chemistry*, the official Journal of IUPAC, in 1969<sup>8</sup>. It was concerned with the measurements, by means of a torsion pendulum, on rigid and toughened PVCs supplied by Solvay and Cie. It also included some impact tests.

This first part was carried out by I. Franta, Technical University of

Prague; J. Heijboer, TNO, Delft; S. Baxter and T. T. Jones, Monsanto Chemicals Ltd, England; G. Pezzin, Montedison, Italy and A. Gonze, Solvay and Cie, Belgium.

While reasonable agreement has been reached for the dynamic mechanical properties, the impact tests varied widely in the rate of elongation and specimen shape and size. No conclusion about correlations could be drawn. The importance of working with samples prepared in one laboratory was pointed out.

The second investigation, using samples prepared by Solvay with rigid and toughened PVCs, was concerned with a more detailed study of the dynamic and standard mechanical properties.

For this further work additional collaborators joined the Working Party: J. Zelinger, Technical University of Prague; M. Chatain, CEMP, Paris; H. Oberst, Farbwerke Hoechst, Germany and W. Retting, BASF, Germany.

This paper summarizes the work done by the working party and the agreement reached in similar experiments, conducted in separate laboratories, on identical materials. A tentative attempt is made to correlate the results of the dynamic mechanical tests with those of the relaxation, tensile and impact tests.

This paper is divided into five sections:

1. Results of dynamic mechanical tests in a wide range of frequencies and temperatures
2. Results of impact tests
3. Results of tensile tests
4. Results of relaxation tests
5. Correlation between the tests

On each diagram, the results of individual participants are identified by means of a roman figure.

- I for BASF
- II for CEMP
- III for Hoechst
- IV for Monsanto
- V for Montedison
- VI for Solvay
- VII for Technical University of Prague
- VIII for TNO

## 1. RESULTS OF DYNAMIC MECHANICAL MEASUREMENTS

### **Materials, equipment and conditions of testing**

All the results obtained in the various laboratories for the dynamic mechanical measurements, during the first and the second part of the work are given here.

The samples used are a rigid PVC (suspension PVC in a lead-cadmium stabilized formula) and the same rigid PVC with 12 parts per hundred (pph) of chlorinated polyethylene (CPE) added.

During the first part of the work, the specimens were prepared in each laboratory from granules furnished by Solvay. For the further work the specimens were cut from sheets prepared in the Solvay laboratory.

Both PVCs, rigid and toughened, were studied at a number of frequencies in the range 0.2 to 2 Hz on a torsion pendulum and in the range 25 to 3700 Hz on devices for the flexural vibration test. For this test four laboratories used the complex modulus apparatus, type 3930, Brüel and Kjaer, Copenhagen. Information about the apparatus and test conditions used by each laboratory is given in *Table 1*.

The measurements on a torsional pendulum are well known. They are described in the ISO recommendation 537. For the flexural vibration experiments on the Brüel and Kjaer device, the specimen is clamped at the upper end, in a vertical position, and is free at the lower end. The free length of the sample varies between 12 and 25 cm depending on the temperature and the frequency. At the lower end, the bar is excited into stationary bending vibrations by means of an electromagnetic transducer. The vibration amplitudes are measured by means of a capacitive or electromagnetic transducer near the clamp.

The resonance frequencies of different order, for a given length of the sample, are measured as well as the half-width of the resonance curve. The loss factor  $d$  equals the quotient of this half-width and the resonance frequency. It is then possible to calculate the storage modulus  $E'$  from the resonance frequency, the free length, the thickness and the density of the bars.

Plots of  $E'$  and  $d$  versus frequency are obtained for each temperature from which values at fixed frequencies are interpolated to give plots of  $E'$  and  $d$  versus temperature.

As for the torsional pendulum measurements, a transition temperature is located by means of the maximum in the curve of  $d$  versus frequency or by means of a dispersion step of  $E'$  which is associated.

For the flexural vibrations the TNO Laboratory used an apparatus described by Dekking<sup>6</sup>. The sample is in an horizontal position and both ends are free.

The dynamic mechanical properties were studied in the various laboratories over a wide range of temperatures from  $-160^{\circ}\text{C}$  to  $+125^{\circ}\text{C}$ .

## Results

A typical plot of storage modulus  $E'$  and loss factor  $d$  or  $\tan \delta$  versus frequency for the rigid PVC in bending vibration is given in *Figures 1.1* and *1.2*. The same plot is given for the toughened PVC in *Figures 1.3* and *1.4*. The curves are given for five participants at about  $20^{\circ}\text{C}$  and  $50^{\circ}\text{C}$ .

*Figure 2* shows the variation of the storage modulus  $E'$  and  $G'$  versus temperature for rigid and toughened PVC at five resonance frequencies, between 1 and 2000 Hz.

Each participant has obtained similar plots for the loss factor and the storage modulus, but the quantitative agreement is not very good. The curves show the lower flank of the so-called  $\beta$  peak of rigid PVC due to a secondary relaxation mechanism in the main molecular chain. At  $20^{\circ}\text{C}$  the maximum of the damping peak is situated at a frequency higher than 2000 Hz. At about 1000 Hz the values obtained by the various participants for the loss factor and the storage modulus vary from  $2.8 \times 10^{-2}$  to  $4.0 \times 10^{-2}$  and from  $3 \times 10^4$  kgf  $\text{cm}^{-2}$  to  $3.8 \times 10^4$  kgf  $\text{cm}^{-2}$  respectively.

Under the same conditions the measurements on the toughened PVC

Table 1. Dynamic mechanical measurements: test conditions and equipment

Contributor	Apparatus	Test method according to ISO No. 533	Material used*	Frequency range (Hz)	Temperature range (°C)	Preparation of test specimens	Dimensions of test specimens (length = free length)
I Retting, BASF	Flexural vibrations, Brüel and Kjaer	Transverse vibration measurements (two ends clamped)	1 and 3	100 to 1000	23, 25 and 53	Sheets, plates and strips from Solvay	153 × 10 × 15 mm
III Oberst, Hoechst	Flexural vibrations, Brüel and Kjaer	Transverse vibration measurements (cantilever beam)	1 and 3	30 to 2000	- 40 to 60	Sheets, plates and strips from Solvay	150 × 10 × 15 mm
IV Barrett and Baxter, Monsanto	Torsion vibration, own construction according to Nielsen	B method	1, 2 and 3	0.2 to 2	- 100 to 50	Granules milled at 170-180°C (thickness 2 mm): sheets pressed at 160°C under 70 kg cm <sup>-2</sup>	5.72 × 0.63 × 0.051 cm and 5.72 × 0.63 × 0.165 gm
V Pezzin, Montedison	Torsion vibrations Flexural vibrations, Brüel and Kjaer	Transverse vibration measurements (cantilever beam)	1 and 3	100 to 1000	- 180 to 125 - 70 to 75	Sheets and strips from Solvay	100 × 10 × 1 mm 170 × 8 × 1.5 mm

## DYNAMIC MECHANICAL AND IMPACT PROPERTIES OF PVC

VI	Gonze, Solvay	Torsion vibrations, Zwick Flexural vibrations, Brüel and Kjaer	A method	1 and 3	0.75 to 2	- 65 to 20	Granules pressed at 190°C under 45 kg cm <sup>-2</sup> Plates pressed at 175°C under 60 kg cm <sup>-2</sup> or extruded	50 × 10 × 0.28 mm 215 and 130 × 10 × 4 mm
VII	Franta, Technical University of Prague	Torsion vibrations, own construction according to Nielsen Nonius torsion vibrations	B method See K. H. Illers and H. Brenar, <i>Kolloid-Z.</i> , 176, 110 (1961)	1, 2 and 3	1 to 1.7	- 60 to 66	Granules pressed at 180°C under 120 kg cm <sup>-2</sup> and relaxed 4 h at 90°C	80 × 10 × 2 mm
VIII	Heijboer, TNO	Nonius torsion vibrations Flexural vibrations, own construction	B method Transverse vibration measurements (free-free beam)	1, 2 and 3 1 and 3	0.2 to 3.2 140 to 3700	- 160 to 70 - 80 to 40	Granules pressed at 185°C under 76 kg cm <sup>-2</sup> (mechanical adjustment of thickness)	150 × 7.02 × 3.52 mm; 50 × 6.5 × 0.51 or 1.65 mm 184.2 × 7.02 × 3.52 mm

\* Materials: 1, rigid PVC; 2, PVC + 6 pph CPE; 3, PVC + 12 pph CPE

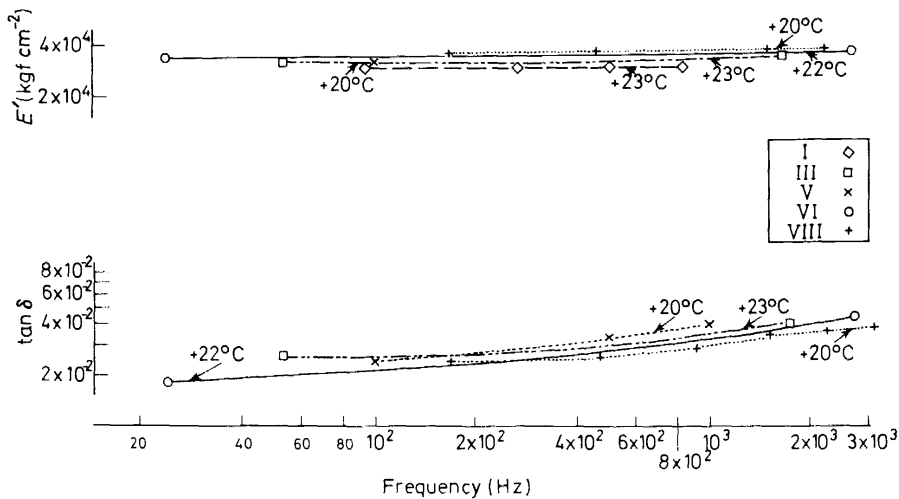


Figure 1.1. Rigid PVC; 20-23°C.

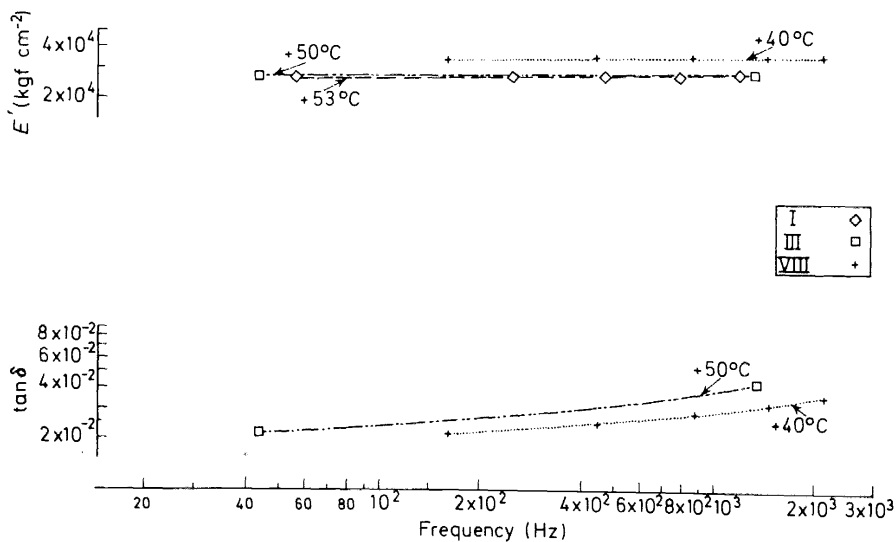


Figure 1.2. Rigid PVC; 40-53°C.

DYNAMIC MECHANICAL AND IMPACT PROPERTIES OF PVC

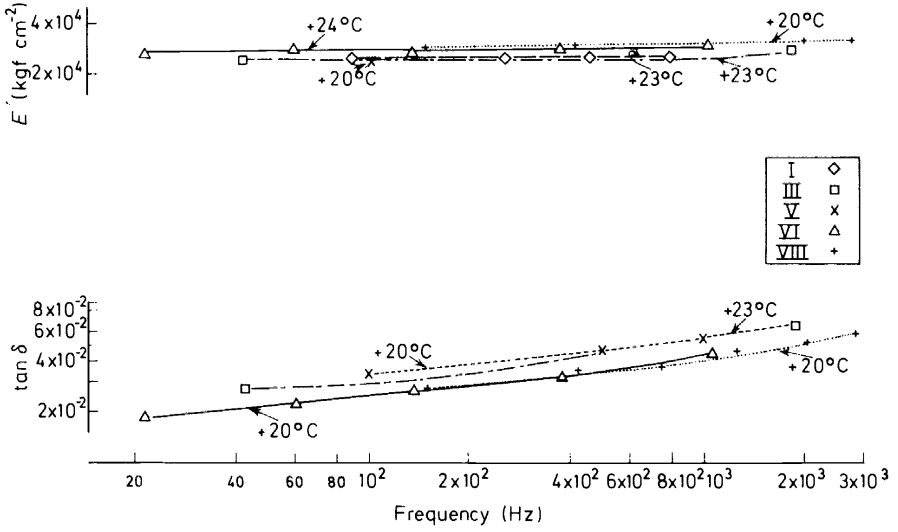


Figure 1.3. Toughened PVC; 20-24 C.

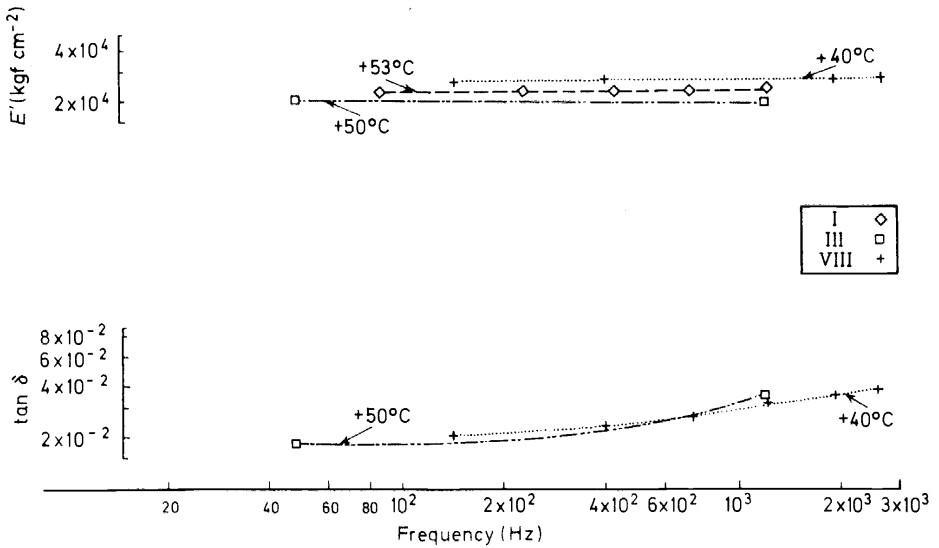


Figure 1.4. Toughened PVC; 40-53°C.



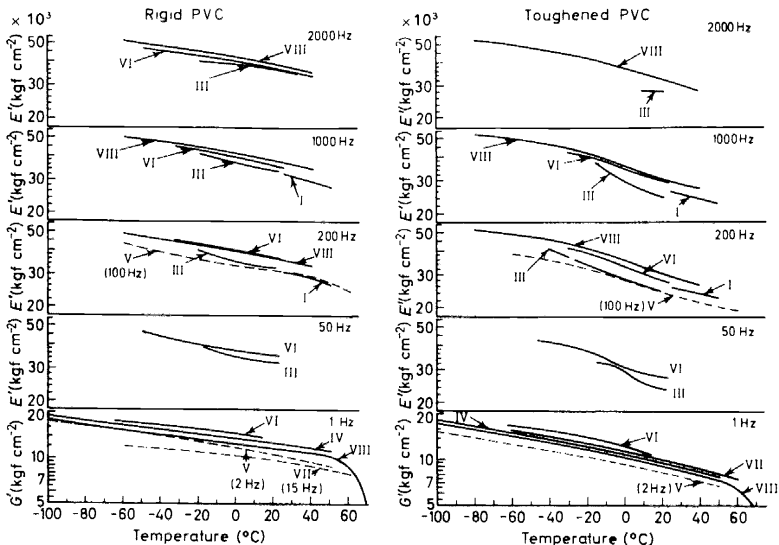


Figure 2.

show a very similar scattering, the damping at about 1000 Hz is found to vary between  $4.1 \times 10^{-2}$  and  $5.5 \times 10^{-2}$  and the storage modulus between  $2.4 \times 10^4$  and  $3 \times 10^4 \text{ kgf cm}^{-2}$ .

Figure 3 represents a plot of the storage moduli  $E'$ ,  $G'$  and the loss factor versus temperature obtained on rigid and toughened PVCs by means of torsional and bending vibrations. The mean shape of the curves are represented at four frequencies 1, 24, 200 and 2000 Hz.

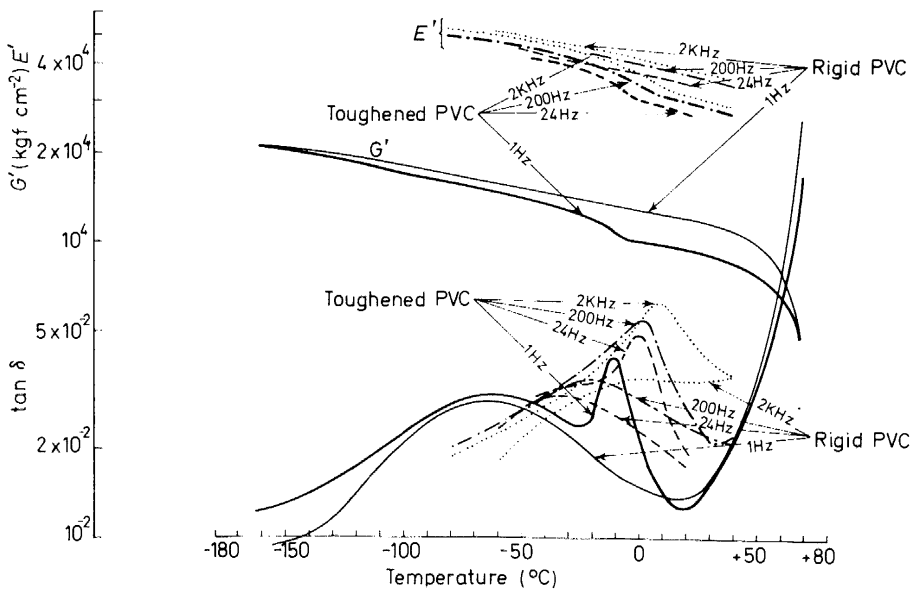


Figure 3.

For rigid PVC the plots show well-known features. For a constant frequency the modulus falls with increasing temperature and steps in the curves can be observed. Associated with these steps we observe, for each frequency, two peaks in the mechanical damping versus temperature. The first one is a broad peak which appears at about  $-60^{\circ}\text{C}$  at 1 Hz,  $-35^{\circ}\text{C}$  at 24 Hz and  $0^{\circ}\text{C}$  at 2000 Hz; the second one is the well-known narrow peak which corresponds to the glass transition of the PVC. The heights of the broad damping peaks are within the range  $2.9 \times 10^{-2}$  at 1 Hz to  $3.4 \times 10^{-2}$  at 2000 Hz.

For toughened PVC, the mechanical damping exhibits a third peak. This narrower peak appears at about  $-10^{\circ}\text{C}$  for 1 Hz. It has been shown in the first part of the work that the height of this peak varies with the amount of CPE present in the PVC. This peak, which corresponds to a very marked dispersion step of  $E'$ , is associated with the relaxation process of the glass-rubber transition of the CPE.

The temperatures at which the damping due to the CPE occurs are significantly dependent on frequency. The temperature of the peak goes from  $-10^{\circ}\text{C}$  at 1 Hz to  $+10^{\circ}\text{C}$  at 2000 Hz. The total height of the rubber damping peak is increased with the frequency but this is probably due to the progressive merging of the broad peak of the PVC into the narrow peak of the CPE when the frequency goes up.

## Discussion

It is known<sup>7</sup> that the temperature dependence of the relaxation time  $\tau$  of each motion of a group of the polymer chain or segments of the chain can be expressed approximately in terms of an apparent energy of activation  $Q$ :

$$\tau \simeq \tau_0 \exp(Q/RT)$$

At any one temperature there will be a whole spectrum of relaxation times, but the large majority will be clustered around a fairly well-defined time and therefore the mean value of the spectrum is considered.

It may be shown that the relaxation time for the material investigated in dynamic mechanical experiments may be equated to the inverse of the circular frequency of the damping peak. Hence for temperatures of maximum damping the frequencies are correlated to the activation energy by the relation:

$$\omega = \omega_0 \exp(-Q/RT)$$

Therefore a plot of  $\ln \omega$  versus reciprocal of absolute temperature should be linear, the slope being  $(-Q/R)$ .

Figure 4 shows the variation of  $\log \nu$  with the inverse of the absolute temperature for the maximum of the secondary relaxation process of PVC and for the rubber damping peak of CPE.

It can be seen that the results obtained by five participants are situated on straight lines for the PVC secondary transition as well as for the transition associated with CPE. The agreement between the experimental values is fairly good.

For the CPE transition temperature the linear relationship obtained is:

$$\ln \nu = -30.070 (T_G)^{-1} + 113.92 \quad \text{with } n = 0.961$$

where  $\nu$  is the frequency in Hz,  $T_G$  is the CPE transition temperature in K and  $n$  is the correlation factor.

The energy of activation,  $Q$ , estimated from all the measurements in the range 0.2 Hz to 2000 Hz, is 60 kcal mol<sup>-1</sup>. This value is equal to that found in the first part of the work on the basis of measurements at low frequencies. This order of magnitude of activation energy is characteristic of a main transition.

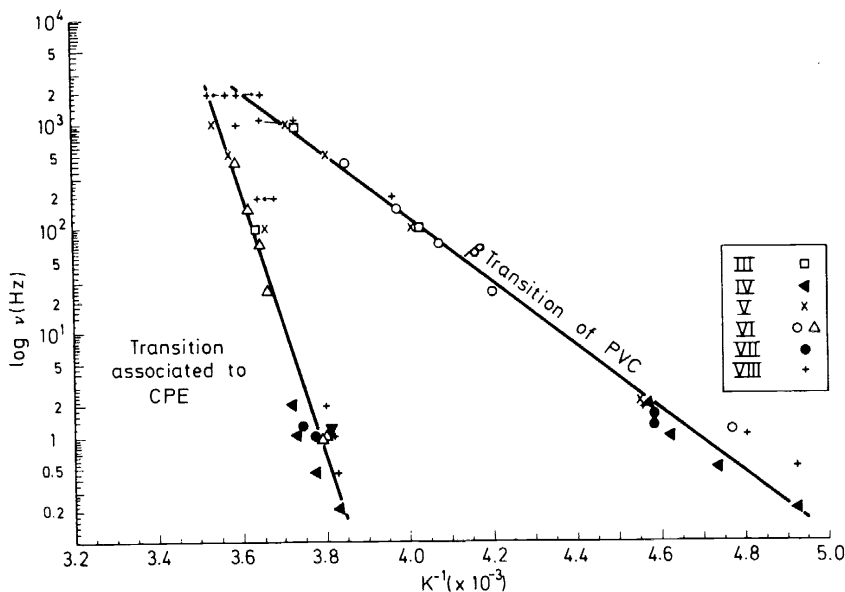


Figure 4.

For the PVC secondary peak, the relationship found is:

$$\ln \nu = -6.917 (T_\beta)^{-1} + 32.5 \quad \text{with } n = 0.993$$

where  $T_\beta$  is the  $\beta$  peak temperature in K.

The points obtained at low frequencies may be divided into two groups which give a higher and a lower value for the activation energy of the  $\beta$  transition. The mean value is 13.8 kcal mol<sup>-1</sup>, extremes being 15 and 13 kcal mol<sup>-1</sup>. This value agrees very well with results published by different workers. It is slightly higher than those found previously (10 to 13 kcal mol<sup>-1</sup>)<sup>8</sup>.

It is possible to make a similar examination of the modulus values at any one temperature for the various frequencies. The discrepancies are more important with regard to the loss-factor determination. It was concluded in the first part of the work that the specimen thickness had some effect on the shear modulus measured in torsional vibrations.

It seems that such an effect is observed in the bending vibrations for which the laboratories have used different thicknesses. The measurements of TNO

and Solvay were carried out with samples of thicknesses of 3.5 and 4 mm. They are in good agreement. Hoechst, BASF and Montedison used thinner samples of 1.5 mm.

The results of the first group are about 10 to 15 per cent higher than those of the second one.

## 2. RESULTS OF IMPACT MEASUREMENTS

### Materials, equipment and conditions of testing

The impact properties of the two PVCs whose dynamic mechanical properties were studied above have been examined. Various kinds of impact tests were applied. The impact strength of the two PVCs was studied over a large range of temperatures and at various rates of deformation.

The test methods and the experimental conditions used by each participant are given in *Table 2*.

### Results and discussion

The results are given in graphical form in *Figures 5, 6 and 7*.

It can be seen from the plots on *Figure 5* that a well-marked brittle-tough transition is observed for all the tests and that the results differ greatly from the rigid PVC to the toughened PVC and from one test to another.

The approximative range of the brittle-tough transition temperatures for rigid and toughened PVC is given in the following table.

Laboratory	Test	Rigid PVC	Toughened PVC
Hoechst	Charpy impact	> 40°C	5-20°C
Monsanto	Falling weight	0-30°C	-5-10°C
Montedison	Izod impact	>40°C	-10-0°C
TNO	Charpy impact	40-45°C	15-20°C
Solvay	Tensile impact	10-15°C	0-5°C
	Prestressed impact	≥ +20°C	0-10°C

As far as we consider only the mean values of the temperatures of the brittle-tough transition for the two materials in the various tests, we notice that the transition temperature of toughened PVC is always 10 to 15°C lower than that for rigid PVC.

For rigid PVC, impact tests carried out with notched pieces exhibit an increase in impact strength at a higher temperature than unnotched pieces, namely, falling weight and tensile impact tests. This is probably due to the fact that the strain conditions are more severe at the root of the notch.

For toughened PVC the result obtained by Montedison in an Izod impact test is not in agreement with this conclusion. The brittle-tough transition is lower in temperature. These differences may be due to the quality of the notch as shown by Oberst<sup>10</sup>.

In attempting to correlate the impact test transition temperatures for notched impact tests, one is faced with the problem of the test pieces being different in size and shape. Some estimate of the strain rate of the test must be arrived at, as has already been discussed in the first paper of the working party on polystyrene<sup>7</sup>.

Table 2. Impact tests: test conditions and equipment

Contributor	Apparatus	Test method	Material used*	Temperature range (°C)	Preparation of test specimens	Dimensions and numbers of test specimens
III Racké, Hoechst	Charpy notched impact	German standard DIN 53453	1 and 3	-40 to 60	Sheets and strips from Solvay	
IV Barrett and Baxter, Monsanto	Falling weight test	British standard 2782, Method 306 B; height of fall constant: 60 and 96 cm; the weight of the striker is varied	1, 2 and 3	-77 to 60	Granules milled at 170°C; sheets pressed at 180°C under 20 kg cm <sup>-2</sup> (thickness 2 mm)	Discs $\phi$ 2.25 in.; thickness 0.06 in; 20 specimens per temper
V Pezzin, Montedison	Zwick pendulum	Test Izod Method: ASTM D-256. Speed: 3.4 m s <sup>-1</sup> ; Energy: 13.8 kg cm	1 and 3	-75 to 68	Sheets and strips from Solvay	63 × 12.7 × 1.5 mm; 12 specimens per temper
VI Gonze, Solvay	Frank pendulum	Method: D 53448 modified. Speed: 3.86 m s <sup>-1</sup> ; Energy: 75 kg cm. Ref.: <i>Plastiques Mod. Elastomères (Paris)</i> , 20(7) (1968)	1 and 3	-20 to 25	Extrusion of sheets	Dumb-bells: narrow section $\approx$ 12 × 5 × 1.5 mm $\approx$ 20 specimens per temper; ASTM D 638-58 T 20 specimens per temper
VIII Heijboer, TNO	Tensile impact test	Method: TNO; Velocity of striker: 3.35 m s <sup>-1</sup>	1, 2 and 3	from -190 to 40	Granules milled at 170°C; sheets pressed at 185°C under 76 kg cm <sup>-2</sup>	Dumb-bells: section 3.2 × 1.3 mm; 4 specimens per temper; 127 (101.6) × 12.7 × 2.3 mm; 2 to 6 specimens per temper
	Charpy notched impact	ASTM D 256 Method B; Speed: 3.35 m s <sup>-1</sup> ; Free length: 4 in	1, 2 and 3	from -190 to 60 (fluid conditioning)		

\* Materials: 1, rigid PVC; 2, PVC + 6 phh CPE; 3, PVC + 12 phh CPE

DYNAMIC MECHANICAL AND IMPACT PROPERTIES OF PVC

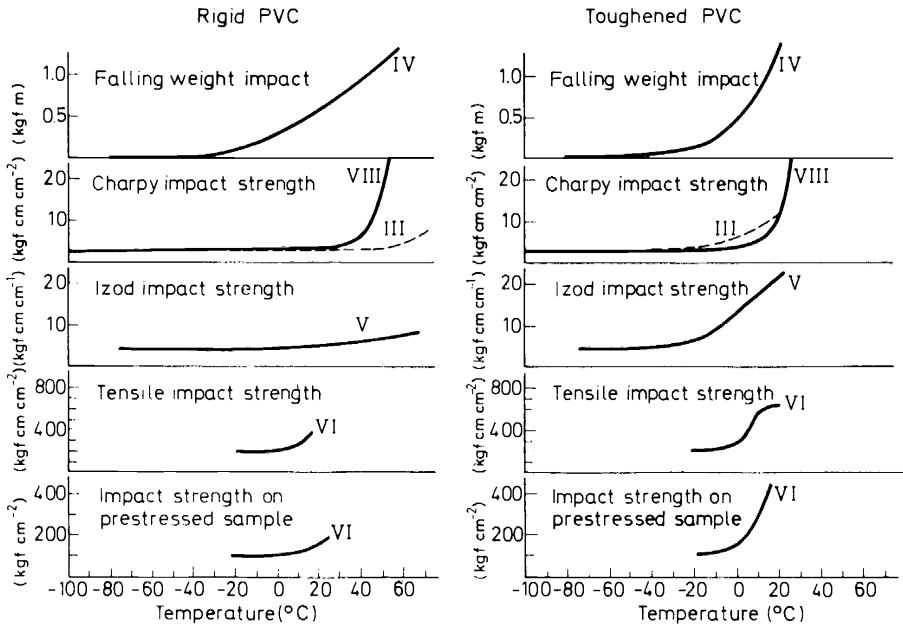


Figure 5.

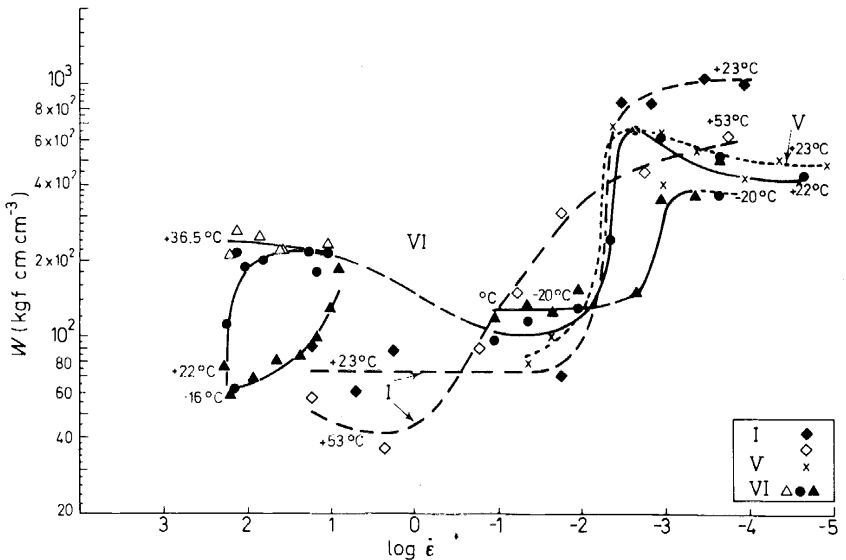


Figure 6. Rigid PVC.

Tensile tests performed at well-defined elongation rates are better suited for a basic study of the ultimate behaviour of solid polymers. Results of tensile tests will be discussed in detail in Section 3 of this report.

In order to allow a direct comparison with the impact tests, the rupture energy values calculated from the tensile measurements are given in *Figures 6 and 7*.

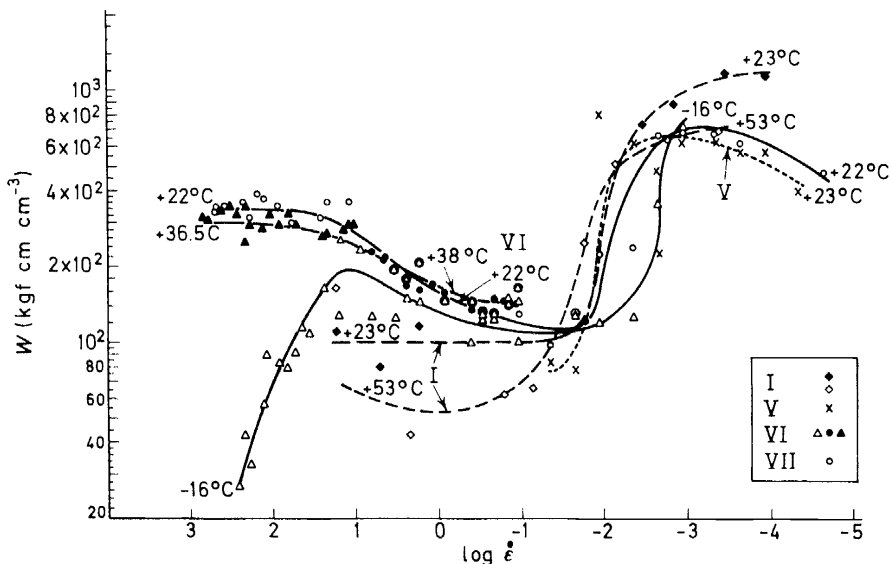


Figure 7. Toughened PVC.

Investigations were carried out in a range of strain rates from  $10^{-5}$  to  $10^2 \text{ s}^{-1}$  and in a range of temperatures from  $-20^\circ\text{C}$  to  $53^\circ\text{C}$ .

For rigid and toughened PVC at about  $20^\circ\text{C}$ , a good agreement exists between BASF, Montedison and Solvay for the position of a first step which is found at about  $5 \times 10^{-3} \text{ s}^{-1}$  for the rigid PVC and  $10^{-2} \text{ s}^{-1}$  for the toughened PVC. This transition is shifted to lower strain rates for lower temperatures.

Solvay has carried out a great number of experiments at the highest strain rates. In the range from  $3 \times 10^{-2}$  to  $10 \text{ s}^{-1}$  the rupture energy increases with the strain rate, because of the increase of the rupture stress. In the range above  $10 \text{ s}^{-1}$  it is seen that a well-marked fall in the rupture energy occurs at  $-16^\circ\text{C}$  and  $+22^\circ\text{C}$  for the rigid PVC and only at  $-16^\circ\text{C}$  for the toughened PVC. It will be seen in Section 3 that these transitions correspond to a sharp decrease in the rupture strain associated with brittle fracture.

In contrast, the first step in the range of low strain rates corresponds to a decrease of the rupture strain in the plastic deformation range (see Section 3).

The CPE rubber is active in both transitions. Its effect is to shift the transitions to the higher strain rates.

Table 3. Tensile tests: test conditions and equipment

Contributor	Apparatus	Test method	Speed range	Material used*	Temperature range (°C)	Preparation of test specimens	Dimensions and numbers of test specimens
I Retting, BASF	Wolpert	Relaxation	$6.7 \times 10^{-4}$ to $10^{-2}$ cm s <sup>-1</sup>	1 and 3	23 and 50	Sheets and strips from Solvay	110(60) × 15 × 1.5 mm: gauge length 40 mm
						Sheets and strips from Solvay	240(200) × 15 × 1.5 mm: gauge length 200 mm
II Chatain, CEMP	Own construction Zwick DY 10	Relaxation	$10^{-4}$ to $3 \times 10^{-3}$ cm s <sup>-1</sup> $3 \times 10^{-3}$ to 1 cm s <sup>-1</sup> 0.1 to 5 m s <sup>-1</sup>	3 3 3	- 40 to 73 - 40 to 73 - 40 to 73	Strips from Solvay	CEMP specimen, dumb-bells
						Strips from Solvay	75(50) × 4 × 1.5 mm
						20, 50 and 60	
III Oberst, Hoechst Grimminger, Hoechst	Instron type TT-CM	Relaxation	1	23, 50, 55, 60, 62 and 70	Sheets and strips from Solvay	(220) × 8 × 1.5 mm 3 specimens per speed and temperature	
		Relaxation	3	23 and 50	Sheets and strips from Solvay		
		Relaxation	1 and 3	22	1.67 × 10 <sup>-3</sup> to 8.33 cm s <sup>-1</sup>		
V Pezzin, Montedison	Instron type TT-CM	ASTM D 638 (+ creep test)	0.05 to 200 mm min <sup>-1</sup>	1 and 3	23	Sheets and strips from Solvay	Gauge length 50 mm
VI Gonze, Solvay	Instron type TT-CM Own construction Frank	ASTM D 638-58 T	0.05 to 500 mm min <sup>-1</sup>	1 and 3	- 42 to 22	Extrusion of sheets	Reference length 75 mm
		ASTM D 638-58 T	0.17 to 58 m min <sup>-1</sup>	3	- 16 to 38	Extrusion of sheets	Reference length 75 mm
		ASTM D 638-58 T	0.5 to 50 m s <sup>-1</sup>	1 and 3	- 16 to 36.5	Extrusion of sheets	Reference length 75 mm



### 3. RESULTS OF TENSILE TESTS IN A VERY LARGE RANGE OF STRAIN RATES AND TEMPERATURES

#### Materials, equipment and conditions of testing

The same PVCs have been used for tensile and impact tests. All the specimens have been cut from extrusion moulded plates and extrusion moulded strips having a thickness of about 1.5 mm.

The experiments were carried out by BASF, CEMP, Hoechst, Montedison and Solvay. Experimental conditions are given in *Table 3*.

The stress relaxation experiments are discussed in Section 4 of this report. They were mainly conducted in the laboratories of BASF and Hoechst.

The experiments of the five laboratories are concerned with tensile tests in the linear region and the non-linear region until fracture.

A very large range of strain rates was covered by means of special devices.

The stress-strain curves were determined in each case. From these curves the following quantities have been measured:

- (a) the Young's modulus in the linear region,  $E$  (kgf cm<sup>-2</sup>)
- (b) the yield stress,  $\sigma_y$  (kgf cm<sup>-2</sup>)
- (c) the yield strain,  $\varepsilon_y$  (per cent)
- (d) the rupture stress,  $\sigma_r$  (kgf cm<sup>-2</sup>)
- (e) the rupture strain,  $\varepsilon_r$  (per cent)
- (f) the rupture energy,  $W_r$  (kgf cm cm<sup>-3</sup>)

The results of the rupture energy measurements, given in *Figures 6* and *7*, have been discussed in Section 2 of this report.

All the results have been plotted versus the strain rate which is the ratio of the crosshead speed to the gauge length of the sample:

$$\dot{\varepsilon} = V/L$$

In some cases, especially for Hoechst and BASF measurements of the relaxation spectra, the results have been plotted versus the yield time and the rupture time which have been calculated from the corresponding elongations and the crosshead speeds.

#### Results

A typical plot of tensile stress-strain curves is given in *Figure 8* for the toughened PVC at  $-16^\circ\text{C}$  for speed of testing from  $0.01 \text{ cm min}^{-1}$  to  $5.71 \times 10^4 \text{ cm min}^{-1}$ . It can be seen that the yield strain passes through a maximum.

#### *Tensile modulus*

*Figure 9* shows the results of the tensile modulus measurements in the linear region. Contributors are BASF and Montedison. The measurements were made up to about 0.5 per cent elongation. The time was calculated by the aid of the ratio  $\Delta L/V$ . The agreement is fairly good between the BASF and Montedison results.

The curves show the shift of the softening region to shorter times when the temperature is increased. This is directly correlated to the main molecular chain mechanisms of PVC (effect of glass transition temperature).

# DYNAMIC MECHANICAL AND IMPACT PROPERTIES OF PVC

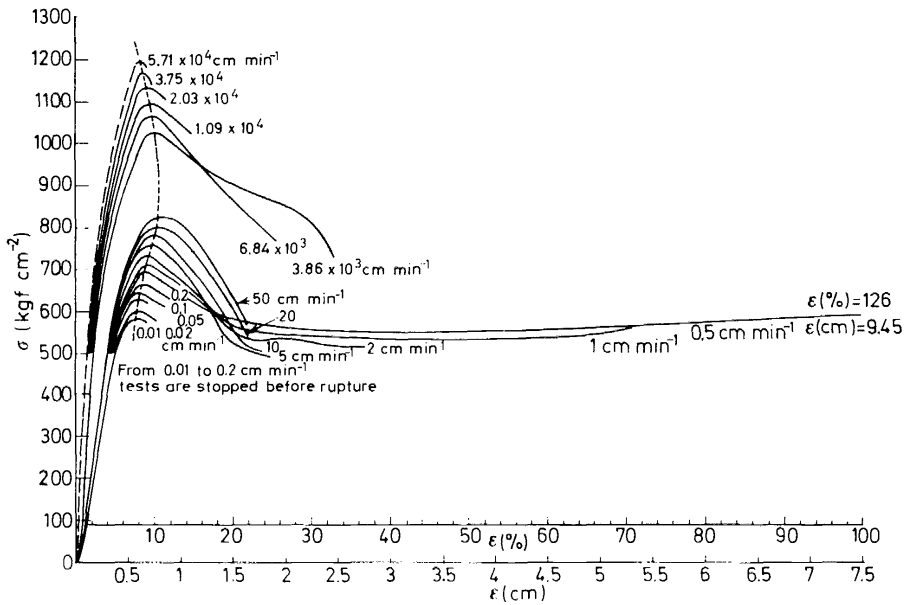


Figure 8. Toughened PVC.

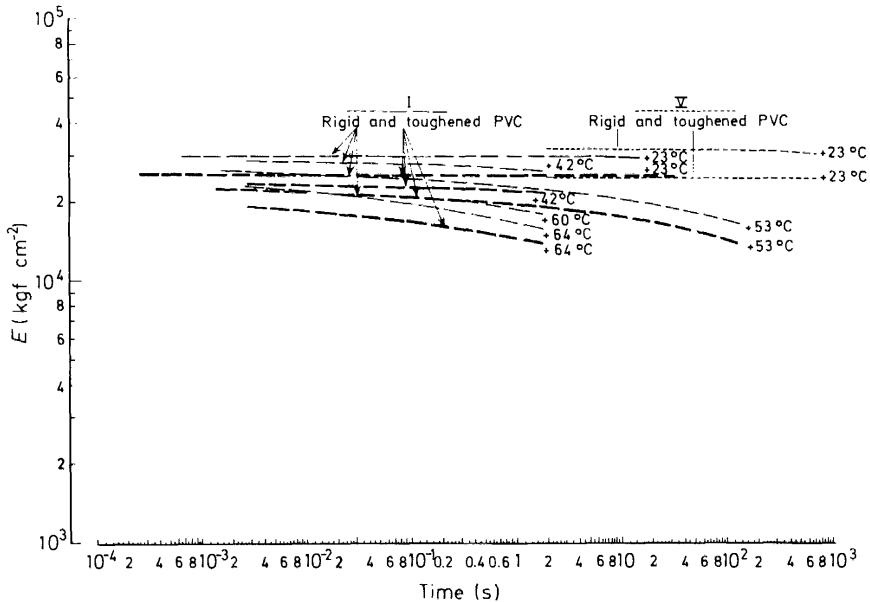


Figure 9.

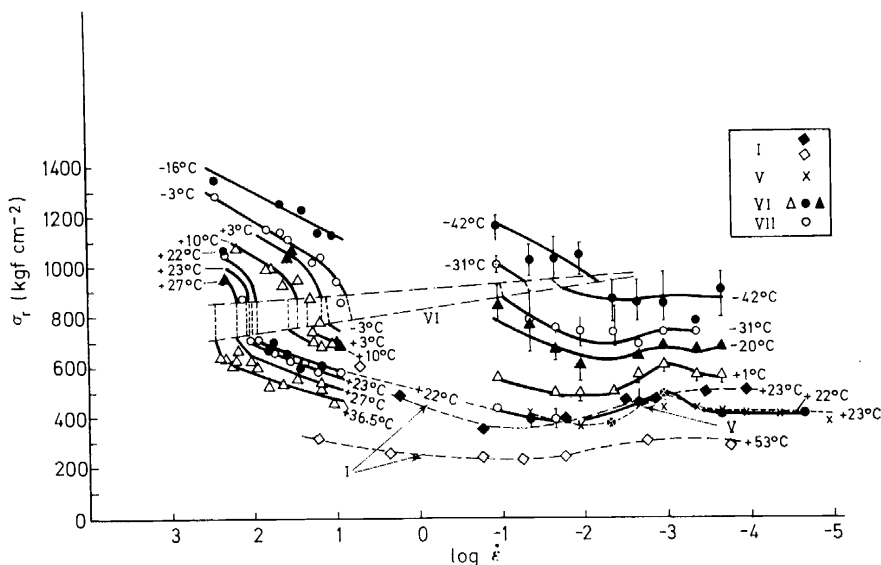


Figure 10. Rigid PVC.

### Rupture stress

Figures 10 and 11 show the values of the rupture stress for rigid and toughened PVC respectively, versus the logarithm of the strain rate. Contributors are BASF, Montedison, Solvay for rigid PVC plus CEMP for toughened PVC.

The curves are characterized by a number of features:

(i) They show a slight minimum at about  $10^{-2} \text{ s}^{-1}$  and give an indication of a maximum at  $10^{-3} \text{ s}^{-1}$ .

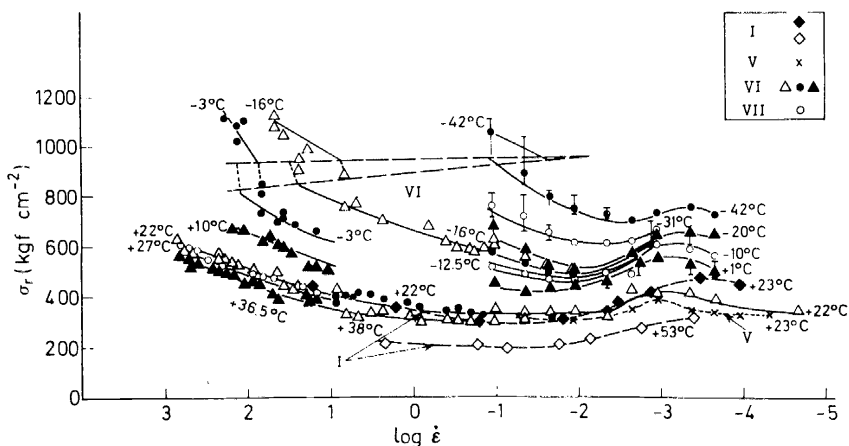


Figure 11. Toughened PVC.

(ii) They show a discontinuity for each temperature after a zone where the rupture stress is increasing with increasing strain rate.

(iii) The strain rate corresponding to this discontinuity is higher, the higher the temperature.

(iv) In the upper part of the figure, the rupture of the samples is brittle for the higher strain rates; the discontinuity corresponds, therefore, to a tough-brittle transition region.

For toughened PVC, the curves are different from those obtained for rigid PVC at the highest strain rates. The ruptures are not brittle for temperatures above 9°C.

Rupture stress of modified PVC is about 20 per cent lower than that for rigid PVC at all the strain rates investigated.

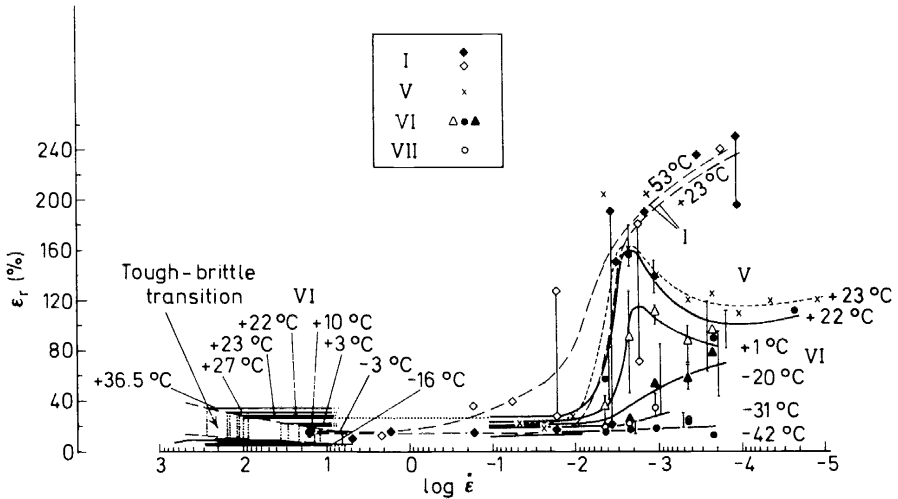


Figure 12. Rigid PVC.

### Rupture strain

Figures 12 and 13 are plots of the rupture strain versus the logarithm of the strain rate for rigid and modified PVC respectively. In several cases the scattering of the measurements has been indicated. Contributors are the same as for the rupture stress measurements.

It is obvious from these plots that the rupture strain does not vary monotonously when the strain rate is increased. Except for very low temperatures ( $-42$  and  $-31^\circ\text{C}$ ), each plot can be divided into three well-defined ranges separated by two transition zones. The rupture strain for toughened PVC at all temperatures is higher than that for rigid PVC.

The agreement between the four collaborators is very good as far as the localization of the strong rupture strain fall is concerned. This fall of ultimate properties situated in the low-speed range indicates that a first variation of the tensile properties in the non-linear range takes place. This zone of variation is slightly displaced, for toughened PVC, to higher strain rates, i.e. to smaller extension times.

After this first variation zone, the rupture strain of rigid PVC (*Figure 12*) keeps constant, at a level dependent on the temperature, for more than three decays of variation of the strain rate. This rupture strain which is three lower than that obtained in the range of lowest strain rates, is still higher than the rupture strains corresponding to a brittle fracture, so that the first variation corresponds to a tough–tough transition.

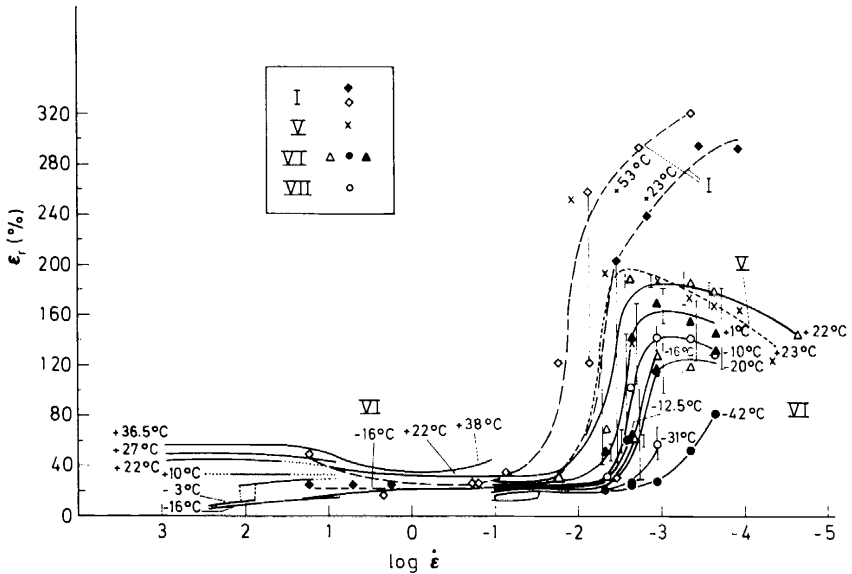


*Figure 13.* Toughened PVC.

If the speed of testing is still increased it is noticed that the rupture strain falls abruptly for a given speed which is different for each temperature, the higher the temperature, the higher the speed. After this fall the rupture strain is reduced in each case to about 6 to 8 per cent and the rupture becomes brittle.

As for the rupture stress, it is possible to define a tough–brittle transition zone in *Figure 12*.

The behaviour is slightly different for toughened PVC (*Figure 13*). In this case, for speeds in the intermediate range, the rupture strain increases for tests above 20°C. The fall at high strain rate is only observed for the tests at lowest temperatures. As for rupture stress the influence of rubber in PVC is visible in the high strain rate region.

Comparing *Figures 10* and *11*, on the one hand, and *Figures 12* and *13*, on the other hand it is obvious that the brittle–tough transition corresponds, for the same strain rates and temperatures, to a sudden fall in rupture strain and a sudden increase in rupture stress.

#### *Yield stress*

*Figures 14* and *15* are plots of the ratio of yield stress to absolute tempera-

DYNAMIC MECHANICAL AND IMPACT PROPERTIES OF PVC

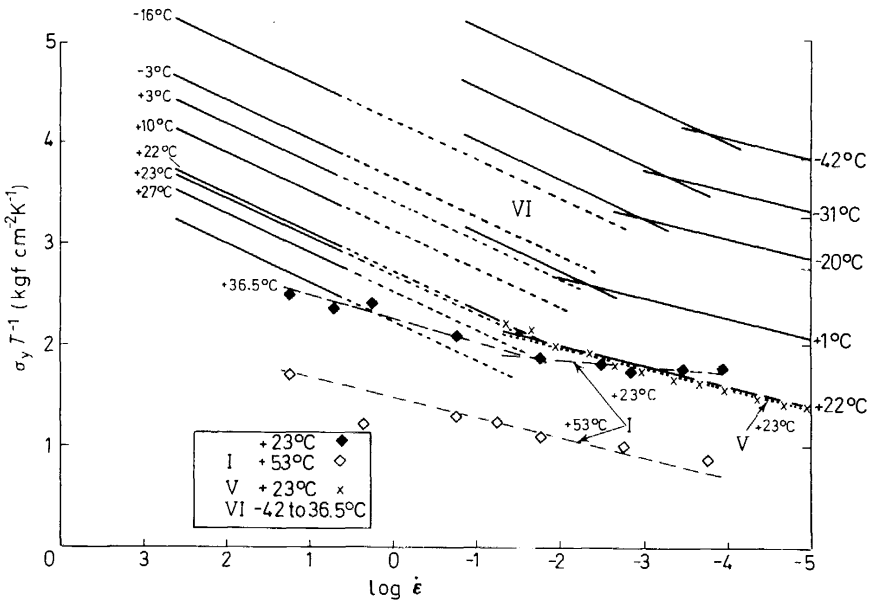


Figure 14. Rigid PVC.

ture against the logarithm of the strain rate. This representation has been chosen in view of the theoretical interpretation of the data, discussed below.

Figure 14 is a comparison, for rigid PVC, of the results obtained by BASF, Montedison and Solvay. Agreement is good at 20–23°C between Montedison and Solvay. The slope for BASF at 23 and 53°C is different. Figure 15 is a similar comparison for toughened PVC.

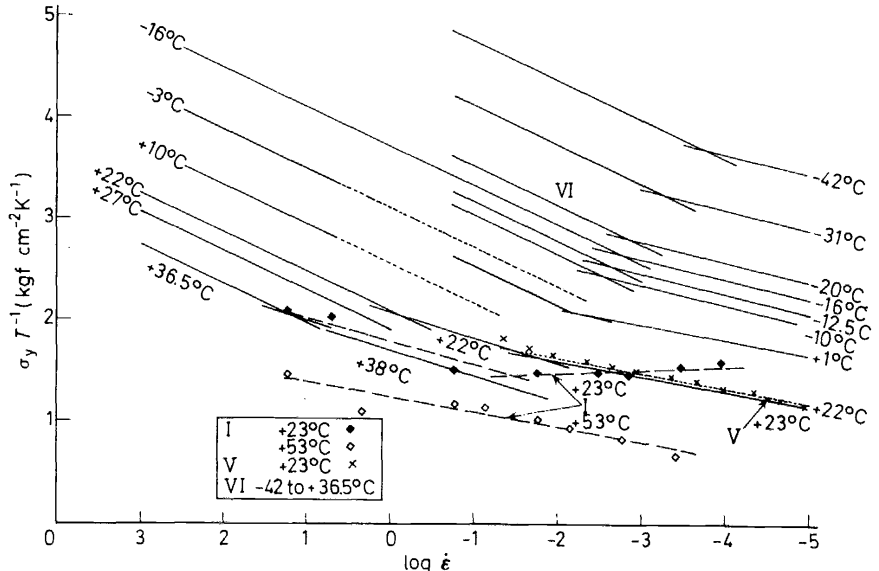


Figure 15. Toughened PVC.

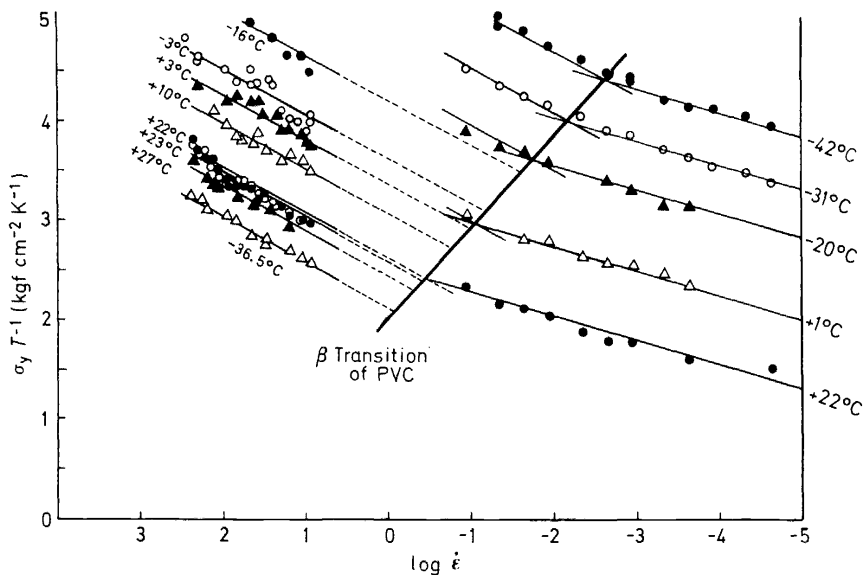


Figure 16. Rigid PVC.

Figures 16 and 17 show only the results from the Solvay Laboratory in a very wide range of strain rates and temperatures. Each point represents one single measurement in the range above  $10 \text{ s}^{-1}$  and the mean value of three tests below  $10 \text{ s}^{-1}$ . The ratio of yield stress to absolute temperature is given against the logarithm of the strain rate. Following Roetling<sup>3</sup> and

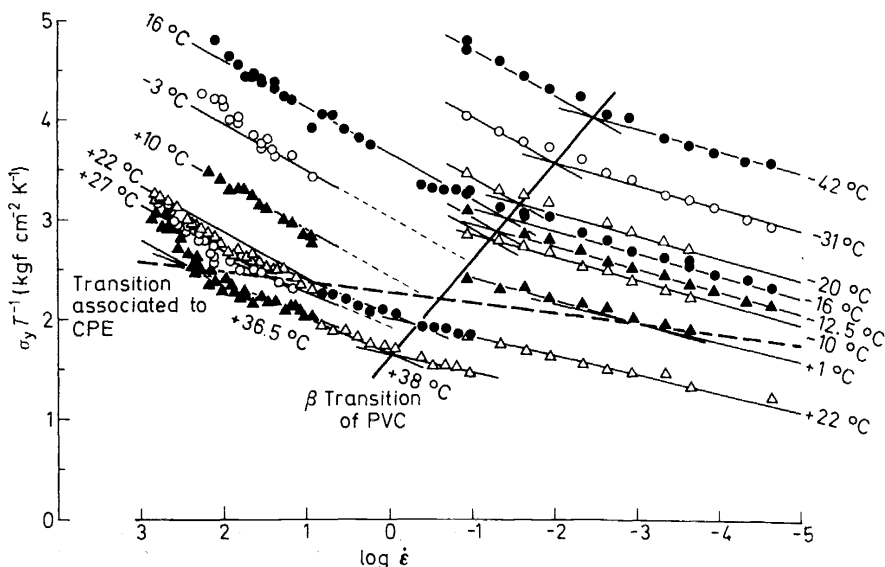


Figure 17. Toughened PVC.

Bauwens<sup>4, 5</sup> the modified or generalized Eyring equation which describes the non-newtonian viscous flow of polymers in the case where two or more deformation processes are involved, has been applied to these data in order to determine whether and how the results would fit this theory over a wide range of experimental conditions.

With the aid of this theory, according to a procedure outlined in the discussion part of this section, the experimental points have been joined in the diagram  $\sigma T^{-1}$  versus  $\log \dot{\epsilon}$  by means of segments of straight lines.

It is obvious from *Figures 16* and *17* that the experimental data may be represented, in a first approximation, by two families of parallel straight lines indicating the presence of two deformation processes: an  $\alpha$  process dominating at high temperatures and low strain rates and a  $\beta$  process whose influence becomes apparent at lower temperatures and for higher strain rates.

Although the number of experimental results is reduced in the zone of high temperature and low speed, it seems that for toughened PVC an additional transition, namely the glass transition of CPE rubber, passes across the two deformation processes of the rigid PVC. The statistical analysis of the experimental data seems to corroborate the existence of this third process, as will be further discussed below.

## Discussion

### *Rupture strain and stress*

The rupture behaviour of PVC gives interesting information on the modes of relaxation in the non-linear range of deformation. As the rupture strain is more sensitive than rupture stress to any modification of test conditions, the variations of the former as a function of temperature and strain rate (*Figures 12* and *13*) were only discussed.

For rigid as well as for toughened PVC two zones of fast variation of rupture strain against strain rate were found.

The first one appears at high strain rates and is temperature dependent. As we wrote above, it is the transition zone between brittle (high speed) and tough (low speed) ruptures of PVC. It disappears at high temperature (22, 27 and 36.5°C) in toughened PVC. This is probably due to an effect of the CPE which prevents brittle ruptures.

An Arrhenius relation can be used to correlate rupture time and temperature in the range of temperatures used, yielding an activation energy of  $14 \pm 2$  kcal mol<sup>-1</sup>. As this value is the same as that found in the dynamic mechanical measurements for the  $\beta$  secondary transition of PVC, we can rightly assume that the brittle-tough transition of PVC in tensile-impact tests is due to the liberation of local motion of the macromolecular chain which allows plastic deformation in the non-linear zone of deformation.

The second transition observed in the rupture strain curves appears at lower strain rates and is slightly temperature dependent (apparent activation energy less than 2 kcal mol<sup>-1</sup>). It is characterized by an important variation in the rupture strain in the tough zone of rupture. Since the deformation process of PVC does not change when the strain rate is increased from values situated, for a given temperature, below the transition zone to values above this transition, and as the temperature dependence of rupture time



at the transition seems rather low, it is not possible to correlate the transition in a straightforward way with the freezing in of a relaxation process of the main molecular chain.

The large variation of rupture strain observed is probably connected with the transition between adiabatic (high rates) and isothermal (low rates) tensile processes.

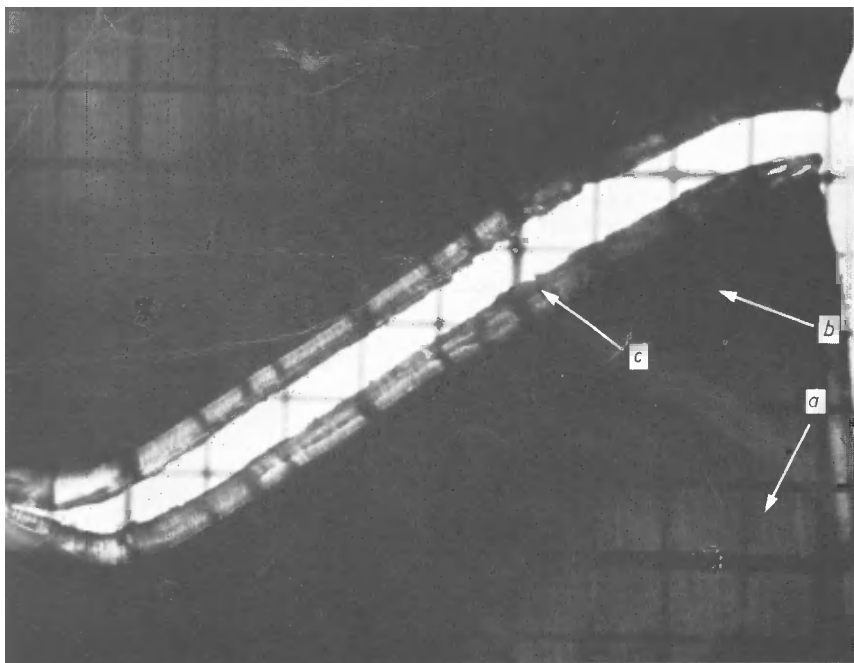


Plate 1. ( $\times 10$ ) Strain rate  $2.2 \times 10^{-2} \text{ s}^{-1}$ : a, undamaged zone; b, zone of plastic deformation; c, zone of fusion.

Plates 1 and 2 show the rupture zones of a transparent PVC tested at two strain rates enclosing the tough-tough transition zone at  $23^\circ\text{C}$ . At strain rates higher than those of the transition (Plate 1), the heat generated by the viscous motion of the matter in the initial zone of deformation cannot be dissipated rapidly enough and an overheating of the PVC takes place.

This local variation of temperature may be high enough to reduce strongly the stiffness of the PVC in a small volume where the deformation is completely localized and give rise to the rupture of the test piece.

As a result of the local overheating, the slight initial plastic deformation formed around the initial zone of deformation cannot propagate in the whole test piece.

On the basis of rupture energy and volume deformation, it has been estimated that the local increase of temperature can be higher than  $100^\circ\text{C}$ . This fact explains the transparency of the lips of the fracture (Plate 1). In this zone, the increase of temperature has been large enough to raise it above

the glass transition temperature of PVC, which explains the local softening of the material.

At strain rates below the transition (*Plate 2*), the heat generated in the initial zone of deformation can be dissipated rapidly enough to prevent a significant increase of temperature. The plastic deformation can propagate in the whole test piece and produces a large rupture strain.

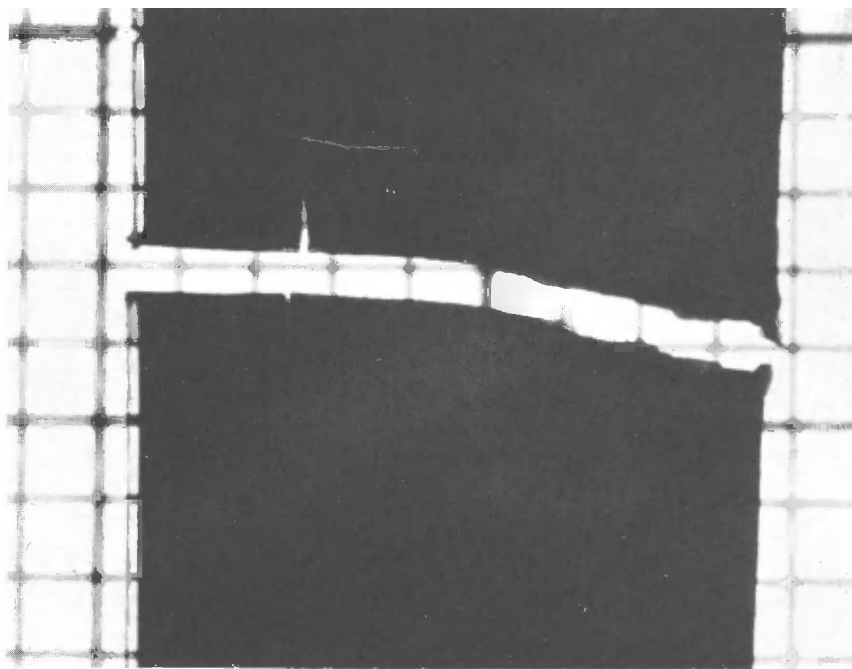


*Plate 2.* ( $\times 10$ ) Strain rate  $1.1 \times 10^{-3} \text{ s}^{-1}$ .

If the proposed interpretation of the observed transition is correct, it may be expected that the latter will be strongly dependent on the rate of heat dissipated in the specimen and would be affected by geometrical factors as, e.g. the thickness of the test piece.

Also, because of the large difference in local and ambient temperatures, the latter cannot be used for a determination of the activation energy.

It is the intention of our Working Party to study these particular points in more detail in the next stage of the programme on the mechanical behaviour of PVC.

#### *Yield stress*

The tensile stress measurements made on rigid and toughened PVC present a maximum which corresponds to a yielding behaviour (yield point). At this point  $d\sigma/dt = 0$  while the strain is increasing. This fact suggests that the deformation behaviour of the rigid and the toughened PVC at this

point is essentially viscous. This behaviour is observed in the glassy range. The yield stress is varying with the temperature and the rate of deformation.

The apparent viscosity of the deformation (ratio of the stress to the strain rate) is usually not constant so that the behaviour is not linear. Application of the Eyring viscosity model to the yield behaviour of glassy polymers has been proposed by various authors<sup>1, 2</sup> and more recently by Roetling<sup>3</sup> and Bauwens<sup>4, 5</sup>.

In the following we will apply the same model to the experimental data of the present report.

The original Eyring equation, applied to the yield stress, may be written in the approximate form:

$$\sigma T^{-1} = A \ln (C\dot{\epsilon}/J) \quad (1)$$

at sufficiently high stress levels, and sufficiently far outside of the transitions, where  $\sigma$  is the yield stress,  $T$  is the absolute temperature,  $A$  and  $C$  are constants,  $\dot{\epsilon}$  is the strain rate and  $J$  is the jump frequency of the rheological unit.

The fundamental process consists of the jump of segments of macromolecules from one equilibrium position to another.

The jump frequency is proportional to the vibration frequency  $J_0$  of the rheological unit and to the probability of a jump when no stress is acting on the material. The probability of a jump is proportional to  $\exp(-Q/RT)$  as required by the Boltzmann distribution law so that

$$J \simeq J_0 \times \exp(-Q/RT)$$

and that equation (1) becomes

$$\sigma T^{-1} = A[\ln(C\dot{\epsilon}/J_0) + Q/RT] \quad (2)$$

where  $Q$  is the apparent activation energy of the process and  $R$  the universal gas constant.

In an extended range of strain rates, the curves  $\sigma T^{-1} = f(\ln \dot{\epsilon})$  do not obey equation (2) but may be represented by at least two segments of straight lines, which according to Roetling and Bauwens correspond to different modes of deformation. The intersection between two segments would correspond to a transition comparable to those revealed by dynamic mechanical measurements. In this case the variation of the yield stress with strain rate and temperature can be described by the generalized theory of non-newtonian viscosity proposed by Ree and Eyring to represent the viscosity of polymer solutions and polymer melts. Following Roetling and Bauwens we suppose that the stresses due to the various processes are additive and that the values of  $A$ ,  $C$  and  $Q$  are constant for a given process. Parameters  $A$  and  $C$  have a structural meaning.

The generalization of equation (2) gives

$$\sigma T^{-1} = \sum A_i (\ln C_i \dot{\epsilon} / J_{0i} + Q_i / RT) \quad (3)$$

At low strain rates the terms containing the variables relating to the other

processes can be neglected. When the strain rate is going up we have to take into account the successive processes.

If one assumes that two processes are involved, equation (3) becomes

$$\sigma T^{-1} = (A_{\alpha} + A_{\beta}) \ln \dot{\epsilon} + \frac{1}{RT} (A_{\alpha} Q_{\alpha} + A_{\beta} Q_{\beta}) + \text{constant} \quad (4)$$

At constant temperature:

$$\sigma T^{-1} = A_{\alpha} \ln \dot{\epsilon} + D_1 \quad (5)$$

in the range between the glass and the secondary transition and

$$\sigma T^{-1} = (A_{\alpha} + A_{\beta}) \ln \dot{\epsilon} + D_2 \quad (6)$$

in the range of strain rates above the secondary transition.

At constant strain rate:

$$\sigma T^{-1} = \frac{A_{\alpha} Q_{\alpha}}{R} \times \frac{1}{T} + D_3 \quad (7)$$

at the highest temperatures and

$$\sigma T^{-1} = \frac{A_{\alpha} Q_{\alpha} + A_{\beta} Q_{\beta}}{R} \times \frac{1}{T} + D_4 \quad (8)$$

for temperatures below the secondary transition.

$D_1$ ,  $D_2$ ,  $D_3$  and  $D_4$  are constants.

These equations show that a plot of  $\sigma T^{-1}$  versus  $\log \dot{\epsilon}$  would give two families of parallel straight lines, the first one with a slope  $A_{\alpha}$  and the second with a slope  $A_{\alpha} + A_{\beta}$ . From the mean displacement of these lines versus temperature, for a given strain rate, it is possible to calculate the activation energies  $Q_{\alpha}$  and  $Q_{\beta}$ .

A plot of  $\sigma T^{-1}$  versus  $T^{-1}$  would also give two families of parallel straight lines with a slope of  $A_{\alpha} Q_{\alpha}/R$  and  $(A_{\alpha} Q_{\alpha} + A_{\beta} Q_{\beta})/R$  respectively.

A similar treatment may be applied to the data on toughened PVC. But in this case a new change of slope (unobserved in rigid PVC) might be involved, corresponding to the glass transition of the chlorinated polyethylene. This process is denoted  $\alpha'$ .

The coefficients of equation (4) have been calculated for the  $\alpha$  and  $\beta$  processes of rigid PVC and for the  $\alpha'$ ,  $\alpha$  and  $\beta$  processes of toughened PVC using a least squares analysis of the experimental data outside the transition zones given by the graphical analysis. Indeed, as may be expected, addition of the experimental values, found in the transition zone, to the statistical analysis, increases the dispersion of the calculated factors.

The results obtained are:

for rigid PVC:

$$\alpha \text{ process} \quad \sigma T^{-1} = 0.106 \ln \dot{\epsilon} + 2683 \frac{1}{T} - 6.57 \text{ kgf cm}^{-2} \text{ K}^{-1}$$

$$\beta \text{ process} \quad \sigma T^{-1} = 0.197 \ln \dot{\epsilon} + 3168 \frac{1}{T} - 8.11$$

for *toughened PVC*:

$$\alpha' \text{ process} \quad \sigma T^{-1} = 0.081 \ln \dot{\epsilon} + 2003 \frac{1}{T} - 4.79$$

$$\alpha \text{ process} \quad \sigma T^{-1} = 0.097 \ln \dot{\epsilon} + 2869 \frac{1}{T} - 7.84$$

$$\beta \text{ process} \quad \sigma T^{-1} = 0.203 \ln \dot{\epsilon} + 3456 \frac{1}{T} - 9.77$$

The activation energies, associated with the various processes, within the 95 per cent confidence interval are:

for *rigid PVC*:

$$Q_{\alpha} = 50.1 \text{ kcal mol}^{-1} \pm 9.5 \text{ kcal mol}^{-1}$$

$$Q_{\beta} = 10.6 \text{ kcal mol}^{-1} \pm 4.5 \text{ kcal mol}^{-1}$$

for *toughened PVC*:

$$Q_{\alpha'} = 49.3 \text{ kcal mol}^{-1} \pm 12.4 \text{ kcal mol}^{-1}$$

$$Q_{\alpha} = 58.2 \text{ kcal mol}^{-1} \pm 11.5 \text{ kcal mol}^{-1}$$

$$Q_{\beta} = 11.1 \text{ kcal mol}^{-1} \pm 4 \text{ kcal mol}^{-1}$$

The differences found between activation energies and parameters for rigid and toughened PVC are of the same order of magnitude as the experimental errors.

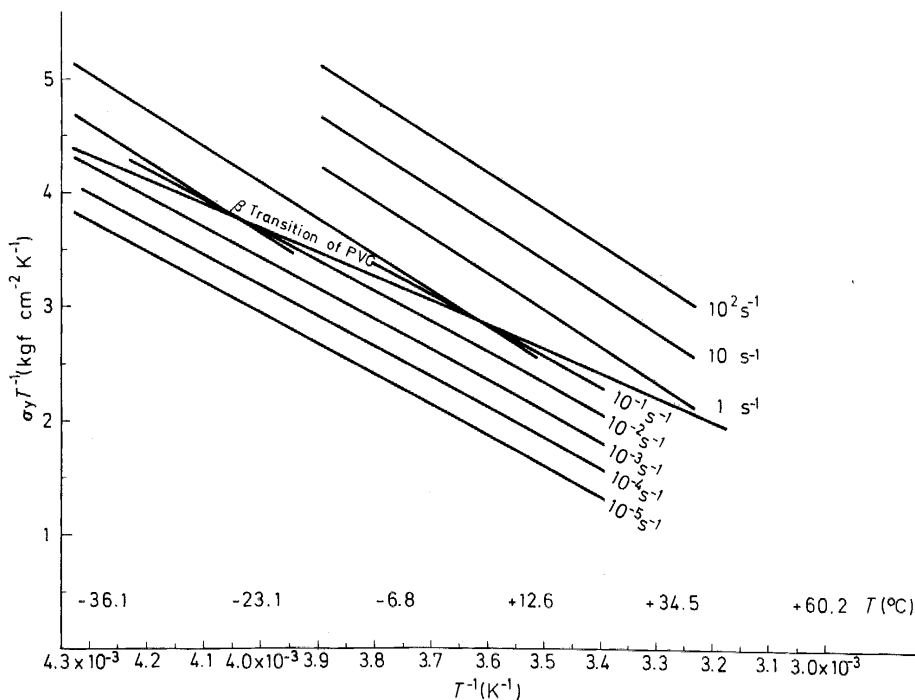


Figure 18. Rigid PVC.

## DYNAMIC MECHANICAL AND IMPACT PROPERTIES OF PVC

For each temperature investigated we have plotted, on *Figures 16 and 17*, the variations of  $\sigma_y T^{-1}$  versus  $\log \dot{\epsilon}$  calculated with the results of the least squares analysis.

The experimental data are generally well represented by the calculated lines. *Figures 18 and 19* show, for a few values of testing speed, the calculated variation of  $\sigma_y T^{-1}$  versus  $T^{-1}$ .

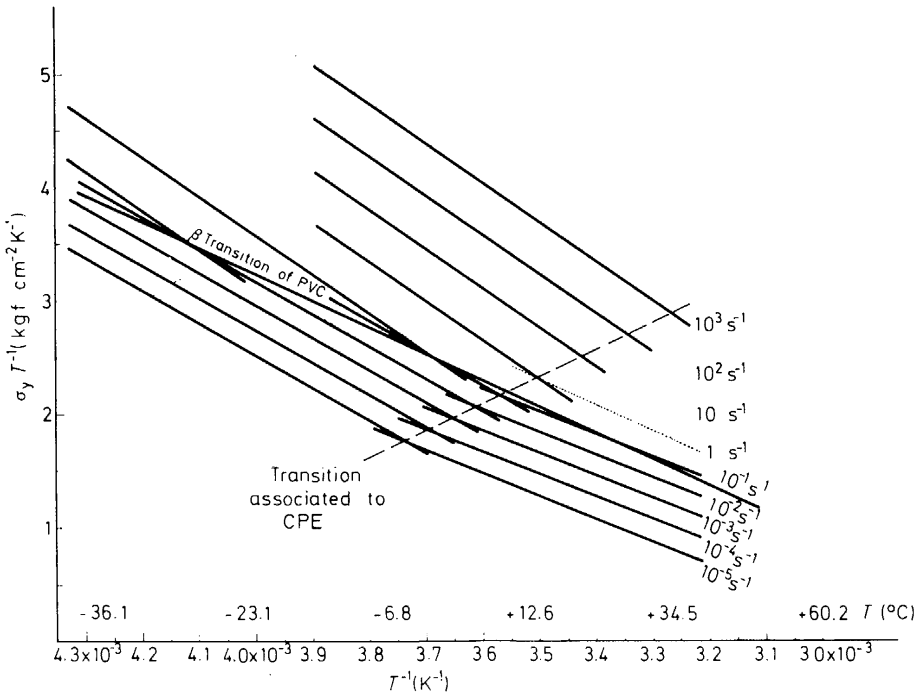


Figure 19. Toughened PVC.

Zitek and Zelinger<sup>11</sup> have applied the same treatment to these experimental data and obtained similar results.

We may conclude, therefore, that the analysis of the experimental data in a broad range of strain rates and temperatures, presented in this report, confirm Bauwens' contention<sup>5</sup> that the  $\beta$  transition in PVC can be revealed, not only by dynamic mechanical or dielectric measurements but also by a detailed study of the yielding behaviour in the glassy state.

The molecular relaxation processes observed in the range of linear viscoelasticity appear, thus, also to influence the non-linear behaviour at large deformations, the technological importance of which is obvious.

## 4. RESULTS OF RELAXATION EXPERIMENTS

The relaxation spectrum of PVC was determined from the following quantities:

(i) The relaxation modulus  $E(t)$  as a function of the measuring time  $t$  in stress relaxation measurements.

(ii) The complex modulus of elasticity as a function of the circular frequency  $\omega = 2\pi\nu$  in flexural vibration experiments.

(iii) The tangential modulus  $d\sigma/d\varepsilon$  as a function of the measuring time in tensile tests.

The measuring methods and the theoretical basis to the experiments are well known. They are described in a paper by Herman Oberst from Hoechst and Wolfgang Retting from BASF<sup>12</sup>.

Figure 9 shows the results of the tensile modulus measurements in the linear region, for BASF and Montedison, versus the measuring time calculated by the aid of the relation  $t = \Delta L/V$ .

Figures 20 and 21 show the results of the relaxation modulus versus relaxation time or measuring time. Contributors are Solvay, 23°C; BASF, 23–42–53–64°C; Hoechst, 23–50–55–60°C. The results of BASF differ from those obtained by Hoechst. These differences may be due to differences in the conditioning of the specimens.

Some results of flexural vibration experiments were presented in Figures 1 and 2 (see Section 1).

The results of the three measuring methods, i.e. the stress relaxation, the tensile and the vibration tests have been summarized in Figures 22 and 23 for the rigid and the toughened PVC respectively. Such a representation allows us to determine the time-dependent modulus  $E(t)$  of viscoelastic substances in a wide range of the time  $t$ .

Considering the fact that the vibration experiments were made on samples differing in shape, size and conditioning, it appears that at 20–23°C the

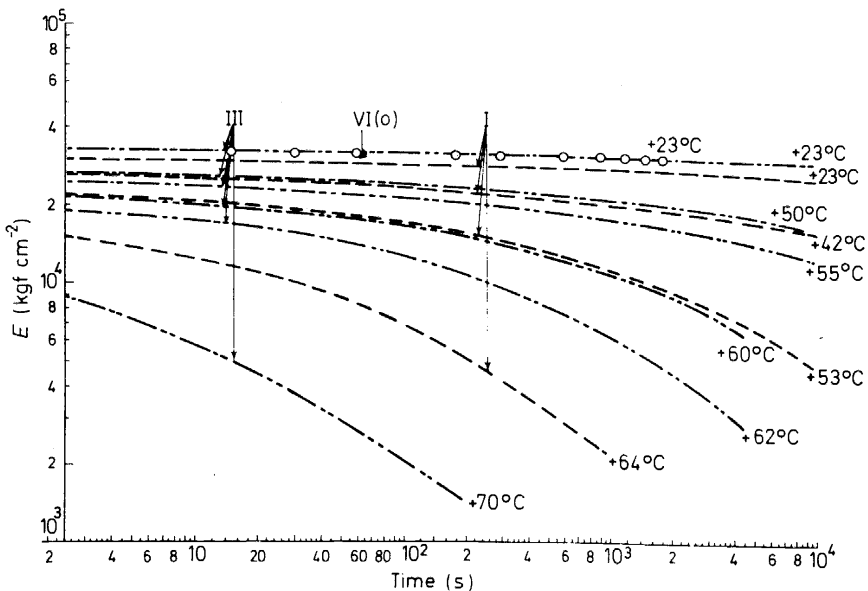


Figure 20. Rigid PVC.

DYNAMIC MECHANICAL AND IMPACT PROPERTIES OF PVC

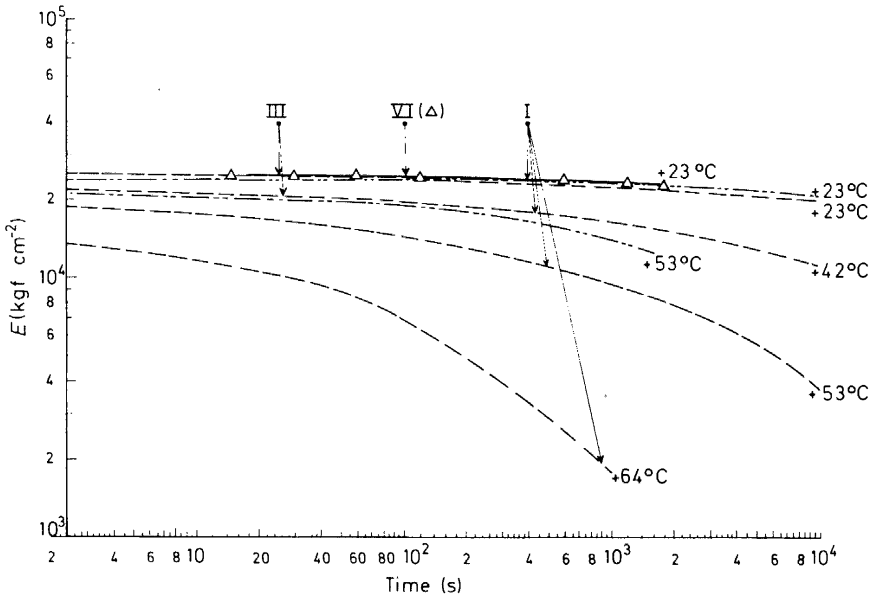


Figure 21. Toughened PVC.

results of the three methods agree reasonably well. The values of the storage modulus at the low-frequency end of the range are similar to those of the tangent modulus for the short time stress strain experiments.

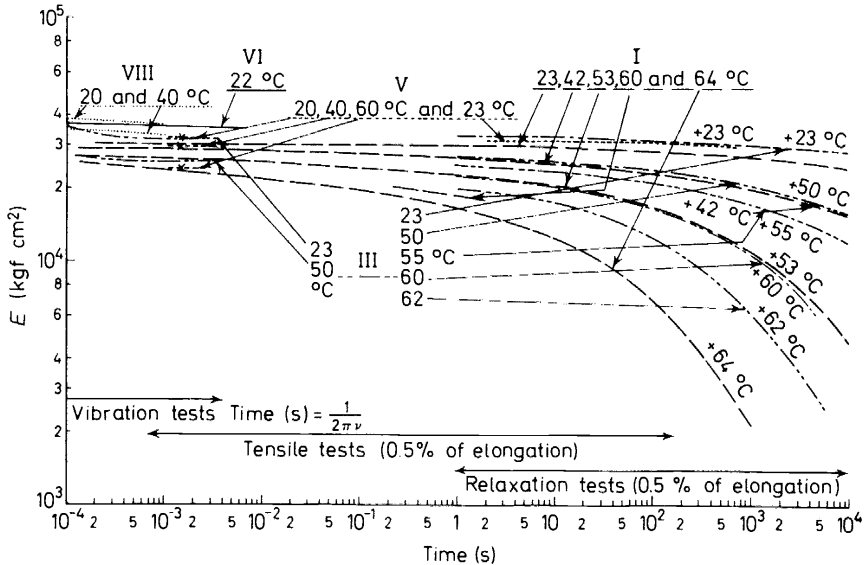


Figure 22. Rigid PVC.



The curves show, for the long times of experiment, the shift of the softening region, corresponding to the glass temperature, to shorter times with increasing temperature. Moreover they show, for the short times of experiment, the lower flank of the so called  $\beta$  peak of the rigid PVC and, for the lowest temperature, the step due to the glass transition temperature of the chlorinated polyethylene.

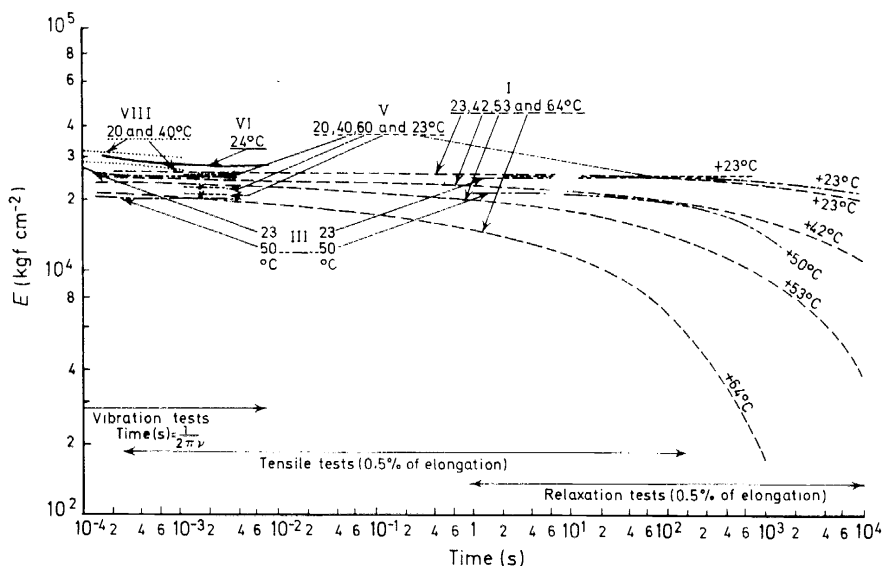


Figure 23. Toughened PVC.

The relaxation spectra  $H(\tau)$  of rigid and toughened PVCs at 23 and 50°C were determined by Oberst and Retting by means of their results of the time-dependent modulus and of the loss modulus  $E''^{12}$ .

A comparison between those curves and the results of the tensile tests in the non-linear range has been presented by Oberst and Retting. For this purpose they have plotted the yield stress, the rupture stress, the rupture strain and the rupture energy versus the yield time and the rupture time respectively and they have related these plots to the relaxation spectra.

Figure 24 is an example of the work done by Oberst and Retting. The relaxation spectra show distinctly that two maxima may be present in a more extended time range, though only the flanks can be observed in the measuring range used.

## 5. STUDY OF THE CORRELATIONS BETWEEN DYNAMIC MECHANICAL, TENSILE, RELAXATION AND IMPACT MEASUREMENTS

The underlying theme of all the studies so far is that the dynamic mechanical, the tensile, the relaxation and the impact measurements are based

DYNAMIC MECHANICAL AND IMPACT PROPERTIES OF PVC

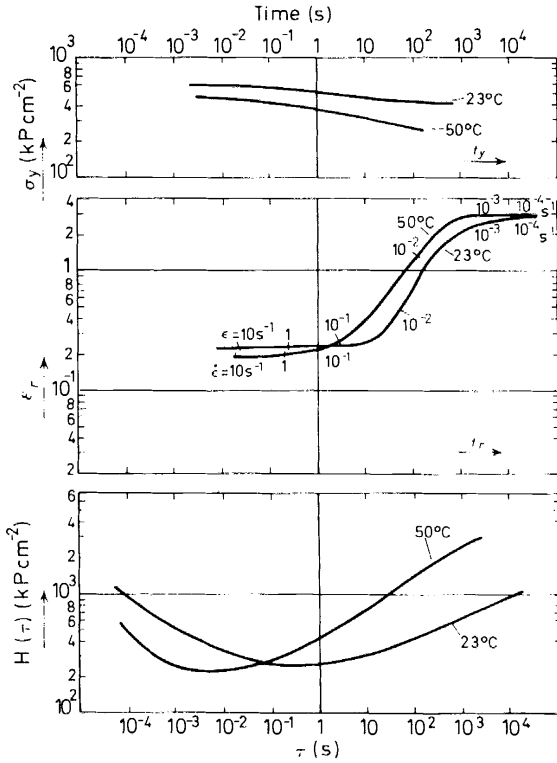


Figure 24. Toughened PVC.

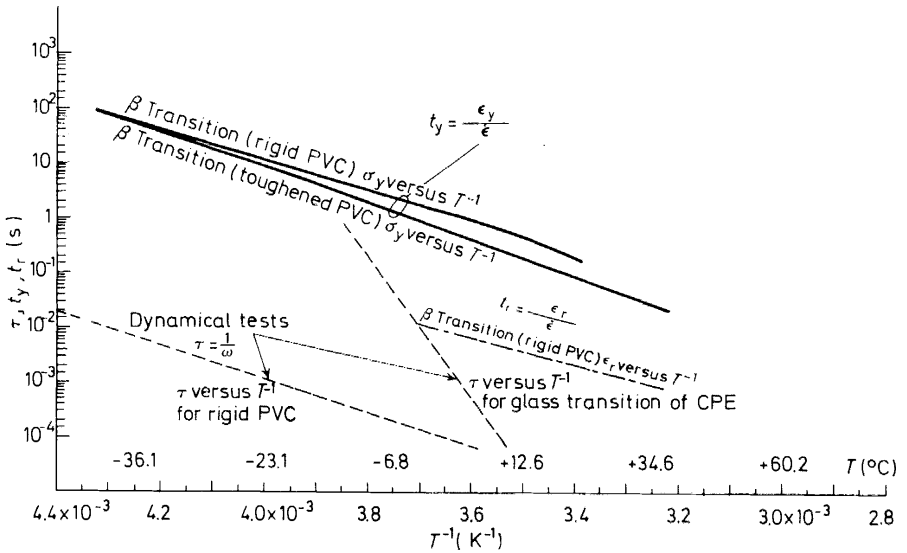


Figure 25.

upon the same relaxation processes possessing different relaxation times. The dispersion regions are met when the frequencies or the strain rates are increased. When the temperature is changed to higher values the relaxation times are all shifted to shorter times so that the dispersion regions in dynamic mechanical, tensile, relaxation and impact measurements are now found at higher frequencies and strain rates, or at shorter times.

The main results we have obtained are summarized in *Figure 4* for dynamic mechanical tests; *Figures 6* and *7* for tensile impact tests; *Figures 10* to *17* for tensile tests, and *Figures 22* and *23* for relaxation tests.

(a) In the *dynamic mechanical tests* at least one secondary dispersion zone takes place, which is named a  $\beta$  transition. The activation energy of this transition is about  $14 \text{ kcal mol}^{-1}$ . *Figure 3* shows that the dispersion secondary peak is very broad and covers  $100^\circ\text{C}$  at low frequency. The temperature of the maximum is shifted from  $-60^\circ\text{C}$  to  $+5^\circ\text{C}$  when the frequency is increased from 1 Hz to 2000 Hz.

The dispersion zone due to the glass transition of the CPE is well marked in the toughened PVC. The corresponding temperatures and frequencies are  $-8^\circ\text{C}$  for 1 Hz and  $+10^\circ\text{C}$  for 2000 Hz.

In *Figure 25* the average relaxation times of the secondary transition and of the CPE glass transition respectively, have been plotted as a function of  $T^{-1}$ . It has already been shown in Section 1 that the apparent activation energies calculated from the slope of these plots, are equal to  $14 \text{ kcal mol}^{-1}$  for the  $\beta$  transition in PVC and  $60 \text{ kcal mol}^{-1}$  for the CPE glass transition.

(b) In *impact and tensile tests*, it has been shown that two transition zones might be involved. The first one, in the low strain-rate range, corresponds to a tough-tough mechanism and is caused or strongly influenced by adiabatic heating of the specimens. Oberst and Retting<sup>12</sup> attributed it to the glass transition of PVC.

The second one, at much higher strain rates, gives rise to a tough-brittle mechanism. Because the time-temperature relation of this transition yields the same value of the activation energy ( $14 \text{ kcal mol}^{-1}$ ) as the  $\beta$  transition measured in dynamic mechanical tests, the tough-brittle transition can be attributed to the same relaxation processes.

The comparison between the usual impact tests and the tensile impact measurements proves that the fracture, in usual impact tests, takes place in the time-temperature range of the  $\beta$  transition.

A transition with the same activation energy has also been found in the yield stress measurements in agreement with the generalized Eyring theory proposed by Bauwens-Crowet<sup>5</sup>.

*Figure 25* allows the comparison of the time-temperature dependence of the transitions measured in the dynamic mechanical and the tensile tests, and illustrates that the 'apparent energies of activation' found for the dynamic mechanical properties, for the rupture behaviour in the brittle-tough transition zone and for the yield stress in tensile measurements are similar.

Although the molecular relaxation processes observed in the range of small deformations also influence the behaviour in the non-linear range, it is clear that the mechanical damping in the linear range and the tensile properties in the non-linear range cannot be connected directly. In particular

the exact location in time of the two transitions in tensile tests cannot be derived from the location of the damping peak. In other words, yield time and rupture time scales cannot be identified with the relaxation time scale found in the linear range of deformation. This conclusion is in agreement with the results of the collaborative study on polystyrene published by Jones<sup>7</sup>.

## REFERENCES

- <sup>1</sup> S. Glasstone, K. J. Laidler and H. Eyring, *The Theory of Rate Processes*, pp 480-483, McGraw Hill, N.Y. (1941).
- <sup>2</sup> R. E. Robertson, *J. Appl. Polymer Sci.*, **7**, 443 (1963).
- <sup>3</sup> J. A. Roetling, Applied Polymer Symposia, No 5, 161-169, Interscience, N.Y. (1967).
- <sup>4</sup> J. C. Bauwens, *J. Polymer Sci., A-2*, **5**, 1145 (1967).
- <sup>5</sup> J. C. Bauwens *et al.*, *J. Polymer Sci., A-2*, **7**, 735 (1969).
- <sup>6</sup> P. Dekking, *PhD Thesis*, Leyden (1961); R. F. S. Hearman, *Brit. J. Appl. Phys.*, **9**, 381 (1958).
- <sup>7</sup> T. T. Jones, *J. Polymer Sci., C*, **16**, 3845 (1968).
- <sup>8</sup> A. Gonze, *Pure and Appl. Chem.*, **18**, 551 (1969).
- <sup>9</sup> A. Gonze, *Plastiques Modernes et Elastomeres*, **20** (7), 134 (1968).
- <sup>10</sup> H. Oberst, *Kunststoffe*, **52**, 4 (1962).
- <sup>11</sup> P. Zitek and J. Zelinger, *J. Appl. Polymer Sci.*, **14**, 1243 (1970).
- <sup>12</sup> H. Oberst and W. Retting, *J. Macromol. Sci. Phys.*, **B**, **5** (3), 559 (1971).